Food Sci. Biotechnol. Vol. 15, No. 6, pp. 871 ~ 876 (2006)

Food Science and Biotechnology

Small and Large Deformation Rheological Behaviors of Commercial Hot Pepper-Soybean Pastes

Su-Jin Choi, Kyoung-Mo Kang, and Byoungseung Yoo*

Department of Food Science and Technology, Dongguk University, Seoul 100-715, Korea

Abstract Rheological behavior of commercial hot pepper-soybean paste (HPSP) was evaluated in small amplitude oscillatory and steady shear tests. Storage modulus (G'), loss modulus (G"), and complex viscosity (η^*) as a function of angular frequency (ω), and shear stress (σ) as a function of shear rate ($\dot{\gamma}$) data were obtained for 5 commercial HPSP samples. HPSP samples at 25°C exhibited a non-Newtonian, shear-thinning flow behavior with high yield stresses and their flow behaviors were described by power law, Casson, and Herschel-Bulkley models. Time-dependent flow properties were also described by the Weltman, Hahn, and Figoni & Shoemaker models. Apparent viscosity over the temperature range of 5-35°C obeyed the Arrhenius temperature relationship with activation energies (Ea) ranging 18.3-20.1 kJ/mol. Magnitudes of G' and G" increased with an increase in ω, while η^* decreased. G' values were higher than G" over the most of the frequency range (0.63-63 rad/sec), showing that they were frequency dependent. Steady shear viscosity and complex viscosity of the commercial HPSP did not fit the Cox-Merz rule.

Keywords: hot pepper-soybean paste, rheology, viscosity, activation energy, dynamic modulus, Cox-Merz rule

Introduction

Hot pepper-soybean paste (HPSP), which is called *kochujang* in Korea, is a popular fermented seasoning sauce. There are two different types of HPSP, which are referred to as traditional and commercial products. The traditional HPSP is prepared from cereal flour, malt flour, fermented soybean starter (*meju*), red pepper powder, salt, and water. The cereal flours used include include rice, glutinous rice, soybean, wheat, or barley. In the preparation of commercial product, *koji*, which is rice or glutinous rice inoculated with *Aspergillus oryzae*, is used instead of *meju* (1). Also, wheat is often used as a fermentation substrate instead of rice or glutinous rice due to its lower price. Corn syrup is also added to most commercial HPSP products to improve their taste and to control the rheological properties of finished products. Recently, consumption of commercial HPSP products has recently grown quite rapidly as people today are not accustomed to the long and complicated preparation process required for traditional HPSP (2), and most consumers also tend to prefer commercial HPSP products due to their better texture, color, taste, and flavor.

The quality of HPSP is determined by changes in the physicochemical, microbiological, and rheological characteristics that are developed through a long period of fermentation. In particular, the rheological properties of HPSP are very important for determining its eating characteristics of the product; it must be thick enough to stay on solid foods (e.g., vegetables), but not so thick for mixing with other food materials (3). The rheological properties also determine the overall mouthfeel of HPSP and influence the intensity of its flavor. Therefore, it is necessary to understand the rheological properties of HPSP that are important for quantifying, predicting, maintaining, and controlling its quality, and also for ensuring its acceptability (1).

HPSP, like other food suspensions, is regarded as shear-thinning fluids with large magnitudes of viscosity and yield stress (1). This non-Newtonian behavior can be attributed to the dispersed solid (red pepper and soybean powder) in a continuous medium and to the presence of high molecular weight substance (starch) in solution. HPSP also exhibits time-dependent flow behavior due to its structure changes that occur during shearing, as noted by Yoo (1) and Choi and Yoo (4). Recently, steady and dynamic rheological properties of traditional HPSP samples have been studied by many researchers. They found that the rheological properties of traditional HPSP depended on fermentation time (3), fermentation temperature (5), concentration (1), mixing ratio of *meju* and rice flours (6), and particle size of red pepper power (7). Although such rheological properties of traditional HPSP were extensively studied, little information is available on the rheological properties of commercial HPSP with the exception of a study of Choi and Yoo (4) who examined the time-dependent flow behavior of commercial HPSP samples. However, no research has examined the detailed dynamic rheological properties of commercial HPSP samples. Therefore, we performed this study to elucidate the rheological properties of commercial HPSP using steady shear sweep and nondestructive dynamic oscillatory measurements.

Materials and Methods

Materials Five commercial hot pepper-soybean pastes (HPSP) collected from different manufactures were obtained from a local supermarket of Seoul, Korea. Each had similar values (59.2-60.0%) for total solid content. In determining the total solid content, HPSP samples were dried in a dry oven at 105°C until they reached a constant

*Corresponding author: Tel: 82-2-2260-3368; Fax: 82-2-2264-3368
E-mail: bsyoo@dongguk.edu
Received July 18, 2006; accepted October 2, 2006

weight. The five samples were then labeled with symbols H1 to H5.

Rheological measurements A TA rheometer (AR 1000, TA Instruments, New Castle, DE, USA) was used to conduct steady and dynamic shear experiments at 25°C using a parallel plate system (4 cm dia.) at a gap 1,000 μm. After loading the rheometer plate, each sample was allowed 5 min to recover its structure and reach the measurement temperature before conducting rheological measurements.

Steady shear data were obtained by measuring shear stress at shear rates ranging from 0.4 to 400 1/sec. To the variations in the steady shear rheological properties of samples, the data were fitted to the well-known power law (Eq. 1), Casson (Eq. 2), and Herschel-Bulkely (Eq. 3) models:

$$\sigma = K\dot{\gamma}^{n} \quad (1)$$

$$\sigma^{0.5} = K_{oc} + K_c\dot{\gamma}^{0.5} \quad (2)$$

$$\sigma = \sigma_h + K_h\dot{\gamma}^{nh} \quad (3)$$

where, σ is the shear stress (Pa), $\dot{\gamma}$ is the shear rate (1/sec), K and K_h are consistency index (Pa·sec^n), n and n_h are the flow behavior index (dimensionless), and σ_h is Herschel-Bulkely yield stress (Pa). Casson yield stress (σ_{oc}) and Casson plastic viscosity (η_c) based on the Casson model (Eq. 2) were determined as $(K_{oc})^2$ and $(K_c)^2$, respectively, that was obtained from linear regression of the square roots of shear rate-shear stress data. Using magnitudes of K and n according to the power law model (Eq. 1), apparent viscosity ($\eta_{a,100}$) at 100 1/sec was calculated. For the study of the influence of temperature on viscosity, the $h_{a,100}$ values were also obtained at different temperatures of 5, 15, 25, and 35°C.

To quantify the time dependency of HPSP samples at a constant shear rate (5 1/sec) and 15°C for 1,000 sec (4), shear stress-time of shearing data were fitted to the Weltman (Eq. 4) (8), Hahn *et al.* (Eq. 5) (9), and Figoni & Shoemaker (Eq. 6) (10) models:

$$\text{Weltman model: } \sigma = A - B \ln t \quad (4)$$

$$\text{Hahn model: } \log(\sigma - \sigma_e) = P - at \quad (5)$$

$$\text{Figoni \& Shoemaker: } \sigma = \sigma_e + (\sigma_{max} - \sigma_e)\exp(-kt) \quad (6)$$

where, σ is the shear stress at time of shearing (t), σ_e is the equilibrium stress value, σ_{max} is the maximum shear stress, and A, B, P, a, and k are constants. Each measurement was taken following a 5-min rest after loading the rheometer, which also allowed for temperature equilibrium.

Dynamic shear data were obtained from frequency sweeps over the range of 0.63-62.8 rad/sec at strain of 3% using small-amplitude oscillation measurements. The 3% strain was in the linear viscoelastic region for each sample. The values of G', G", η^*, and tan δ as a function of frequency, were calculated using TA rheometer Data Analysis Software (version VI.1.76). The measurements were repeated at least three times to ensure their reproducibility. Results reported are an average of the three measurements.

Results and Discussion

Steady shear properties Tables 1 and 2 show the magnitudes of rheological parameters from the power law, Casson, and Herschel-Bulkley models, which were used to describe the flow curves of commercial HPSP samples (Fig. 1). Experimental data of shear stress (σ) and shear rate ($\dot{\gamma}$) in the temperature range of 5-35°C were fitted well to three models (Eq. 1-3) with high determination coefficients (R^2 = 0.97-0.99) in describing the steady shear rheological properties of HPSP samples. All samples at 25°C had shear-thinning behavior with values of flow behavior indices of n_h = 0.59-0.68 and n = 0.34-0.40 which were higher than those (n = 0.24-0.31) found in traditional HPSP (1). The higher n values found in this study may be due to the presence of corn syrup in the commercial HPSP products. However, the flow behavior index values obtained from the power law and Herschel-Bulkely model did not change much between samples at 25°C. According to Yoo (1), the shear-thinning behavior of HPSP can be attributed to solid particles (red pepper powder and soybean power) and a high molecular weight substance (starch) that were dispersed together in the liquid, as observed in other food suspensions. Especially, such shear-thinning behavior of HPSP seems to be mainly influenced by the presence of the solid particle aggregation that results from as a result of the particle-particle interaction that intensifies with increase in the number of aggregated particles, as described by Lee *et al.* (6). They also stated that the number of aggregated particles decreases as the shear rate increases, resulting in the shear-thinning behavior of HPSP.

The steady shear rehological data show that the magnitudes of parameters (K, K_h, $\eta_{a,100}$, η_c, and σ_{oc}) obtained from all three flow models decreased with increasing temperature, except for σ_h with high standard deviation values, in which there was no particular trend as compared to σ_{oc} values, as shown in Tables 1 and 2. In general, it has been known that the intermolecular distance increases with increasing the temperature, which results in lower viscosity and yield stress. The HPSP samples also exhibited high magnitudes

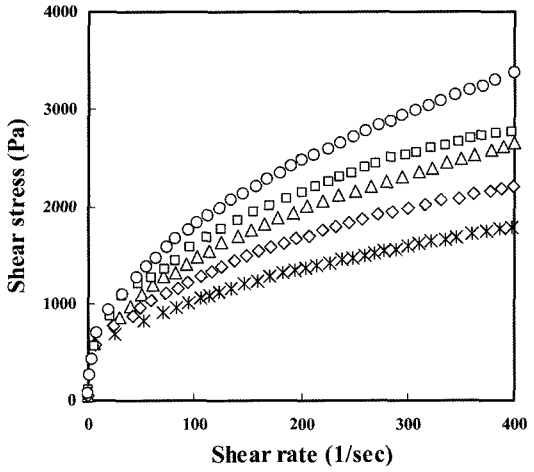

Fig. 1.Shear rate-shear stress plots for commercial HPSP samples at 25°C. (*) H1, (△) H2, (◇) H3, (□) H4, (○) H5.

Table 1. Power law model parameters and apparent viscosity of commercial HPSP samples at 5, 15, 25, and 35°C.

Sample	Temperature (°C)	Apparent viscosity	Power law model		
		$\eta_{a,100}$ (Pa·sec)	n (-)	K (Pa·sec^n)	R^2
H1	5	21.6±0.54	0.33±0.00	453±3.28	0.99
	15	14.5±0.88	0.32±0.00	339±2.46	0.98
	25	10.4±0.13	0.34±0.00	218±0.21	0.99
	35	7.58±0.58	0.33±0.00	162±0.18	0.98
H2	5	30.1±1.72	0.36±0.01	545±0.48	0.99
	15	19.0±0.74	0.35±0.01	380±5.07	0.99
	25	14.7±0.02	0.36±0.00	278±0.81	0.99
	35	10.5±0.36	0.36±0.00	189±2.17	0.99
H3	5	27.3±0.91	0.36±0.01	509±4.11	0.99
	15	18.1±0.80	0.35±0.00	362±7.55	0.98
	25	13.5±0.51	0.38±0.00	234±1.42	0.99
	35	9.75±0.39	0.35±0.00	197±2.60	0.97
H4	5	31.0±1.73	0.34±0.00	665±3.83	0.99
	15	20.2±0.16	0.33±0.00	435±1.99	0.99
	25	15.7±0.09	0.34±0.00	323±1.55	0.99
	35	11.5±0.22	0.35±0.00	232±1.40	0.98
H5	5	36.5±1.20	0.40±0.00	581±0.43	0.99
	15	24.6±0.47	0.39±0.00	408±2.55	0.99
	25	17.6±0.58	0.40±0.00	279±1.28	0.99
	35	12.7±0.24	0.40±0.00	206±3.61	0.99

of σ_{oc} and σ_h which were in the range of 295-1048 and 329-635 Pa, respectively (Table 2). This indicates that there were substantial differences between all parameter values for all HPSP samples. Such differences between HPSP samples might be due to several factors such as the manufacturing process, the content of ingredients (i.e., cereal, hot pepper powder, and corn syrup), and the type of cereal used for the preparation of HPSP. From these observed results, it could be concluded that the commercial HPSP samples studied were shear-thinning fluids with high magnitudes of yield stresses over a temperature range of 5-35°C, and that they showed different steady shear rheological properties.

Effect of temperature on apparent viscosity Various temperatures are often encountered during the storage of commercial HPSP, which makes understanding the effect of temperature on their rheological properties very important. Therefore, we examined the effect of temperature (5-35°C) on apparent viscosity ($\eta_{a,100}$) at a specified shear rate using the Arrhenius equation (Eq. 7), in which the apparent viscosity decreases to an exponential function with temperature. We have experimentally confirmed the Arrhenius temperature relationship in previous studies, which we found high determination coefficients for traditional HPSP samples (1, 6).

$$\eta_{a,100} = A \cdot \exp(Ea/RT) \quad (7)$$

where, $\eta_{a,100}$ is the apparent viscosity (Pa·sec) at 100 1/sec, A is a constant (Pa·sec), T is the absolute temperature (K), R is gas constant (8.3144 J/mol·K), and Ea is the activation energy (kJ/mol). The magnitudes of Ea and A were determined at each concentration from regression analysis of 1/T vs. ln $\eta_{a,100}$, as shown in Fig. 2. The calculated values of Ea and constant A were in the range of 18.3-20.1 kJ/mol and 0.85-1.88×10^{-2} Pa·sec, respectively, with the

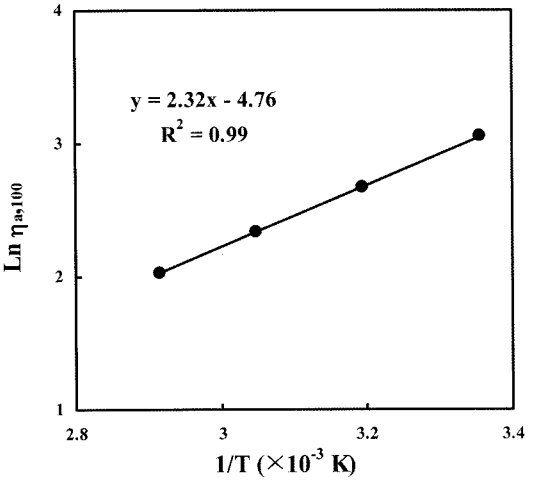

Fig. 2. Apparent viscosity ($\eta_{a,100}$) at 100 1/sec as a function of temperature for sample H1.

Table 2. Casson model and Herschel-Bulkley model parameters at 5, 15, 25, and 35°C.

Sample	Temperature (°C)	Casson model			Herschel-Bulkely model			
		σ_{oc} (Pa)	η_c (Pa·sec)	R^2	n_h (-)	K_h (Pa·sec^n)	σ_h (Pa)	R^2
H1	5	794±3.30	3.00±0.09	0.99	0.48±0.01	174±22.6	562±8.41	0.99
	15	552±8.41	2.12±0.38	0.98	0.66±0.03	41.9±9.64	612±31.8	0.98
	25	393±0.68	1.46±0.06	0.99	0.68±0.00	25.3±0.05	455±9.60	0.99
	35	295±4.40	1.01±0.01	0.98	0.69±0.00	19.2±4.87	329±17.3	0.98
H2	5	1014±16.7	5.08±0.46	0.99	0.47±0.00	288±9.80	550±20.4	0.99
	15	651±9.77	3.27±0.69	0.98	0.54±0.00	126±10.1	472±12.3	0.99
	25	458±1.97	2.67±0.09	0.99	0.64±0.00	51.1±0.61	501±1.70	0.99
	35	342±15.8	2.00±0.21	0.99	0.77±0.00	16.3±1.07	463±38.8	0.98
H3	5	865±9.12	4.96±0.13	0.99	0.49±0.00	232±12.6	517±18.3	0.99
	15	625±5.48	2.83±0.11	0.99	0.63±0.03	64.7±13.0	635±44.5	0.98
	25	434±0.91	2.29±0.13	0.98	0.63±0.00	49.0±1.92	480±10.1	0.99
	35	333±5.34	1.65±0.27	0.99	0.80±0.01	14.3±3.65	447±34.6	0.97
H4	5	1041±8.87	5.21±0.44	0.99	0.43±0.00	364±12.8	552±34.6	0.99
	15	725±13.9	3.34±0.15	0.99	0.47±0.01	167±6.36	534±15.5	0.98
	25	498±4.42	2.80±0.10	0.99	0.59±0.00	69.1±0.16	510±5.02	0.98
	35	366±2.05	2.10±0.07	0.98	0.75±0.01	20.5±4.12	470±27.5	0.98
H5	5	1048±26.6	7.99±0.33	0.99	0.49±0.00	316±4.31	569±29.5	0.99
	15	731±20.7	5.29±0.07	0.99	0.56±0.02	145±5.90	566±12.6	0.98
	25	504±4.16	3.92±0.08	0.99	0.66±0.00	60.5±2.76	519±18.2	0.99
	35	370±1.74	2.70±0.12	0.99	0.79±0.00	21.0±3.33	500±10.3	0.99

Table 3. Activation energies (Ea) of commercial HPSP samples

Sample	A ($\times 10^{-2}$ Pa·sec)	Activation energy (kJ/mol)	R^2
H1	0.85	19.4	0.99
H2	1.11	19.5	0.99
H3	1.09	19.4	0.99
H4	1.88	18.3	0.99
H5	1.08	20.1	0.99

high determination coefficients (R^2 = 0.99) (Table 3), showing that the HPSP samples had varying sensitivities to the increase in temperature. The Ea value (18.3 kJ/mol) of sample H4 was relatively lower than those (19.4-20.1 kJ/mol) of other samples. This suggests that the decrease in viscosity with temperature was more pronounced at sample H4. According to product label information, all HPSP products had been manufactured with wheat as their fermentation substrate, except for sample H4 which contained a mixture of glutinous rice and wheat. It has been known that glutinous rice plays important role in stable network structure of HPSP during storage (7). Yoo (11) also reported that Ea values of glutinous rice flour dispersions (5-8% concentration) were in the range of 11.2-11.9 kJ/mol, and there was no change much with the appreciable effect of concentration on Ea. This indicates that Ea values of HPSP products that contain glutinous rice are lower than those of commercial HPSP samples (H1, H2, H3, and H5) without glutinous rice. Therefore, it can be concluded that a low Ea value, as seen in sample H4, may be due to the presence of glutinous rice in HPSP.

Time-dependent flow behavior and application on models The relationship between shear-stress and time of shearing at a constant shear-rate of 5 1/sec was determined for all HPSP samples (Fig. 3). Similar to Shoemaker and Figoni (12), a characteristic viscoelastic behavior in the typical time-dependent curves of all samples was observed with two distinct regions: one comprised between the onset of shear and the maximum shear stress (σ_{max}) (stress build-up region), and another delimited by σ_{max} and the equilibrium stress value (σ_e) (stress decay region). According to the time-dependent curves in the stress decay region, it is obvious that the shear stress decreased rapidly, occurring in the first few minutes of treatment. Later, the decrease became slower until the sample reached an equilibrium shear-stress value. Experimental values in the stress decay region were fitted to three models (Weltman, Hahn, and Figoni & Shoemaker. Eq. 4-6) (Table 4). Both the Weltman model (R^2 = 0.97-0.99) and the Hahn model (R^2 = 0.97-0.98) fitted the time-dependency data better than did the Figoni & Shoemaker model (R^2 = 0.91-0.97). This is in good agreement with the results of Choi and Yoo (4), who found that both Weltman and Hahn models were more applicable for

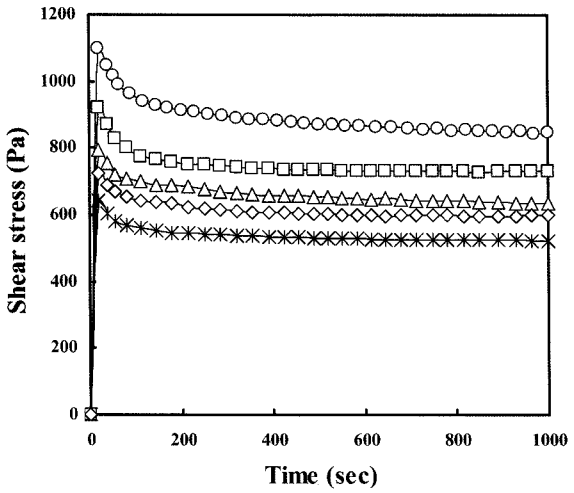

Fig. 3. Time-dependent curves for commercial HPSP samples at 25°C and 5 1/sec. (*) H1, (△) H2, (◇) H3, (□) H4, and (○) H5.

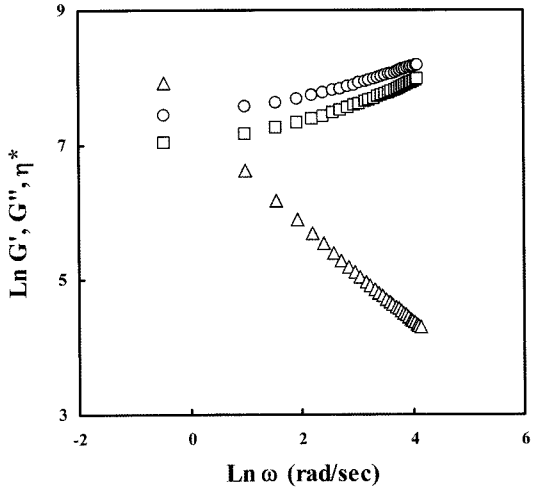

Fig. 4. Plot of ln G', G", η* vs. ln ω for sample H1 at 25°C. (○) G', (□) G", (△) η*.

traditional HPSP samples at various shear rates (5-35 1/sec) and temperatures (5-25°C). The magnitudes of parameters obtained from these three models also varied for the commercial HPSP samples, as shown in Table 4.

Dynamic shear properties Figure 4 shows changes in storage modulus (G'), loss modulus (G"), and complex viscosity (η*) as a function of the frequency (ω) for a typical commercial HPSP sample (H1) at 25°C. The magnitudes of G' and G" increased with an increase in ω, and G' was higher than G" at all values of ω, which showed a slight frequency dependency. Ln η* versus ln ω plot shows shear-thinning behavior following power law model. This behavior is in good agreement with those found in traditional HPSP samples (1, 3, 5, 7). Table 5 shows that the dynamic moduli (G', G", and η*) of sample H4 were higher than those of other samples, indicating that the viscoelastic properties of sample H4 can be increased by the addition of glutinous rice, as described previously. Such higher dynamic moduli can be also attributed to the high viscoelasticity of added glutinous rice, which is concentrated within the liquid phase in the HPSP, due to its thickening properties.

In relation to structure, ln (G', G") versus ln ω plots of weak gels have positive slopes and G' is greater than G" over a wide range of ω, as indicated by Ross-Murphy (13). As shown in Fig. 4 and Table 5, it was found that all samples displayed weak gel-like behavior because the slopes of G' and G" are positive and the magnitudes of G' (1.53-2.05 kPa) are higher than those of G" (1.11-1.41 kPa) at 6.3 rad/sec, showing that the G"/G' ratio (tan δ) is in the range of 0.68-0.75. These results suggest that all samples are more elastic than viscous. Such tan d values at 6.3 rad/sec were much higher than that (tan δ=0.34) of the traditional HPSP (14), indicating that the viscous properties of the commercial HPSP samples may be increased mainly by the presence of corn syrup which is not used to prepare the traditional HPSP. It was also found that there was not much difference between tan δ values of all samples. Therefore, it could be concluded that there were a little differences of dynamic rheological properties

Table 5. Storage (G') and loss (G") moduli, complex viscosity (η*), and tan δ at 6.3 rad/sec of commercial HPSP samples at 25°C

Sample	G' (kPa)	G" (kPa)	η* (kPa·sec)	Tan δ
H1	1.99±0.02	1.36±0.00	0.38±0.00	0.68±0.00
H2	1.67±0.02	1.23±0.00	0.24±0.01	0.74±0.01
H3	1.55±0.01	1.11±0.01	0.30±0.00	0.72±0.00
H4	2.05±0.01	1.41±0.01	0.39±0.01	0.69±0.00
H5	1.53±0.00	1.16±0.00	0.30±0.00	0.75±0.00

Table 4. Parameters from the Welman, Hahn, and Figoni & Shoemaker models for commercial HPSP samples at 25°C.

Sample	Weltman model			Hahn model			Figoni & Shoemaker model		
	A	B	R^2	a ($\times 10^2$)	P	R^2	$\sigma_{max} - \sigma_e$	k ($\times 10^2$)	R^2
HP1	602±1.91	38.0±1.80	0.98	0.79±0.01	2.11±0.04	0.97	110±0.70	1.90±0.00	0.95
HP2	994±2.97	67.3±0.84	0.98	0.65±0.07	2.26±0.01	0.98	161±5.60	2.00±0.00	0.96
HP3	840±12.3	64.5±1.05	0.99	0.90±0.00	2.14±0.01	0.97	118±0.11	2.30±0.00	0.93
HP4	1012±3.50	69.1±1.33	0.99	0.85±0.21	2.28±0.02	0.98	164±2.60	2.30±0.01	0.91
HP5	1205±0.30	72.7±1.64	0.97	0.90±0.28	2.41±0.02	0.98	223±14.0	1.90±0.01	0.97

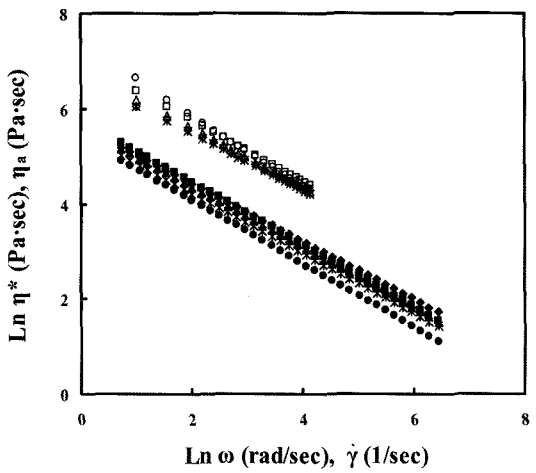

Fig. 5. Comparison of steady flow viscosity (η_a) and complex viscosity (η^*) for (○) H1, (△) H2, (*) H3, (□) H4, and (◇) H5. Open symbol: η^*, closed symbol: η_a.

between the commercial HPSP samples tested.

Correlation between complex and apparent viscosity The empirical Cox and Merz rule (15) proposes that the magnitudes of complex viscosity (η^*) and apparent viscosity (η_a) must be superimposed at equal values of frequency (ω, rad/sec) and shear rate ($\dot{\gamma}$, 1/sec) (Eq. 8).

$$\eta^*(\omega) = \eta_a(\dot{\gamma})|_{\omega=\dot{\gamma}} \quad (8)$$

where, η^* is the complex dynamic viscosity (Pa·sec) and η_a is the steady shear apparent viscosity. When the Cox-Merz rule is followed, it can predict the steady shear properties of a material from their dynamic rheological properties obtained without extensive alteration of its structures (16). To examine the applicability of the Cox-Merz rule, η_a and η^* of the commercial HPSP samples were presented as functions of $\dot{\gamma}$ and ω, respectively (Fig. 5). It was observed that the magnitudes of η^* were greater than those of η_a, as in the most of cases, indicating that the Cox-Merz rule was not applicable to the commercial HPSP samples. This inapplicability could be attributed to the structure decay that often results from the effect of the strain deformation that is applied to the system (i.e., low strain in oscillatory shear and high strain in steady shear), as described by Chamberlain and Rao (17). In the present study, the obvious deviation of Cox-Merz rule could be also explained by the elastic gel-like structure of the commercial HPSP products, which occured the pronounced η^* values over the range of frequency (16, 18). Similar results have previously been observed in traditional HPSP samples (3) and other food suspensions (19, 20). These observations show that the Cox-Merz rule could not directly describe the relationship between dynamic and apparent viscosity for the commercial HPSP samples.

Acknowlegments

This work was supported by Korea Research Foundation Grant funded by the Korean Government (MOEHRD) (KRF-2005-041-F00068).

References

1. Yoo B. Rheological properties of hot pepper-soybean paste. J. Texture Studies 32: 307-318 (2001)
2. Lee DS, Jang JD, Hwang YI. The effects of using packaging films with different permeabilities on the quality of Korean fermented red pepper paste. Int. J. Food Sci. Technol. 37: 255-261 (2002)
3. Yoo B, Choi WS. Effect of fermentation time on rheological properties of *kochujang* in steady and dynamic shear. Food Sci. Biotechnol. 8: 300-304 (1999)
4. Choi SJ, Yoo B. Time-dependent flow properties of commercial *kochujang* (hot pepper-soybean paste). Food Sci. Biotechnol. 14: 413-415 (2005)
5. Yoo B, Noh WS. Effect of fermentation temperature on rheological properties of traditional *kochujang*. J. Korean Soc. Food Sci. Nutr. 29: 860-864 (2000)
6. Lee SM, Lim IJ, Yoo B. Effect of mixing ratio on rheological properties of *kochujang*. Korean J. Food Sci. Technol. 35: 44-51 (2003)
7. Yoo B, Lee SM, Chang YH. Rheological properties of *kochujang* as affected by the particle size of red pepper powder. Food Sci. Biotechnol. 10: 311-314 (2001)
8. Weltman RN. Breakdown of thixotropic structure as a function of time. J. Appl. Phys. 14: 343-350 (1943)
9. Hahn SL, Ree T, Eyring H. Flow mechanism of thixotropic substances. Ind. Eng. Chem. 51: 856-857 (1959)
10. Figoni PI, Shoemaker CF. Characterization of time dependent flow properties of mayonnaise under steady shear. J. Texture Studies 14: 431-442 (1983)
11. Yoo B. Steady and dynamic shear rheology of glutinous rice flour dispersions. Int. J. Food Sci. Technol. 41: 601-608 (2006)
12. Shoemaker CF, Figoni PI. Time-dependent rheological behavior of foods. Food Technol.-Chicago 38: 110-112 (1984)
13. Ross-Murphy SB. Rheological methods. pp. 138-199. In: Biophysical Methods in Food Research. Chan HWS (ed). Blackwell Sci. Pub. London, UK (1984)
14. Choi SJ, Yoo B. Rheological effect of gum addition to hot pepper-soybean pastes. Int. J. Food Sci. Technol. 41: in press (2006)
15. Cox WP, Merz EH. Correlation of dynamic and steady viscosities. J. Polm. Sci. 28: 619-622 (1958)
16. Da Silva PMS, Oliverira JC, Rao MA. Rheological properties of heated cross-linked waxy maize starch dispersions. Int. J. Food Properties 1: 23-34 (1998)
17. Chamberlain EK, Rao MA. Rheological properties of acid converted waxy maize starches in water and 90% DMSO/10% water. Carbohyd. Polym. 40: 251-260 (1999)
18. Rao MA, Okechukwu PE, Da Silva PMS, Oliveira JC. Rheological behavior of heated starch dispersions in excess water: role of starch granule. Carbohyd. Polym. 33: 273-283 (1997)
19. Bistany KL, Kokini JL. Dynamic viscoelastic properties of foods in texture control. J. Rheol. 27: 605-620 (1983)
20. Rao MA, Cooley HJ. Rheological behavior of tomato pastes in steady and dynamic shear. J. Texture Studies 23: 415-425 (1992)